nature research

https://doi.org/10.1038/s41567-020-01152-5

Supplementary information

Quantum diffusion of microcavity solitons

In the format provided by the authors and unedited

Supplementary Information for "Quantum diffusion of microcavity solitons"

Chengying Bao,[1] Myoung-Gyun Suh,[1] Boqiang Shen,[1] Kemal Şafak,[2] Anan Dai,[2] Heming Wang,[1] Lue Wu,[1] Zhiquan Yuan,[1] Qi-Fan Yang,[1] Andrey B. Matsko,[3] Franz X. Kärtner,[4,5] and Kerry J. Vahala[1,*]
[1]T. J. Watson Laboratory of Applied Physics, California Institute of Technology, Pasadena, California 91125, USA.
[2]Cycle GmbH, Hamburg 22607, Germany.
[3]Jet Propulsion Laboratory, California Institute of Technology, Pasadena, California 91109, USA.
[4]Center for Free-Electron Laser Science, Deutsches Elektronen-Synchrotron, Hamburg 22607, Germany.
[5]Department of Physics and the Hamburg Center for Ultrafast Imaging, University of Hamburg, Hamburg 22761, Germany.
[6]Present address: Physics & Informatics Laboratories, NTT Research, Inc. 940 Stewart Dr, Sunnyvale, California 94085, USA.
*Corresponding author: vahala@caltech.edu

1. Calibration of the BOC signal

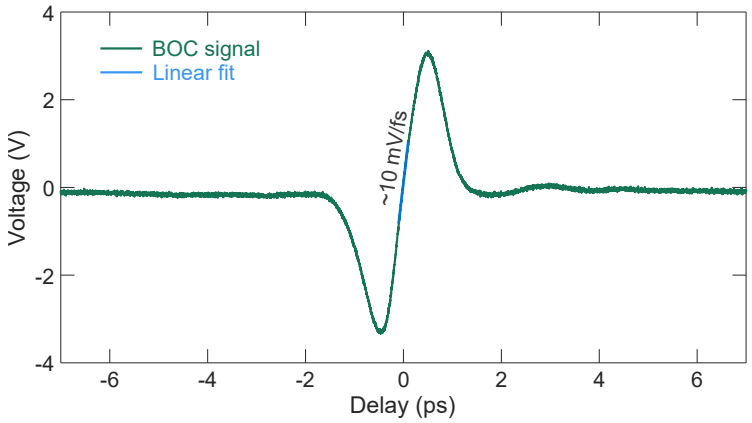

FIG. S1: **Calibration of the BOC signal.** The green line is the BOC signal when the delay between the two inputs was scanned. A linear fit around the zero-crossing region gives the discrimination slope.

Figure S1 is an example of the BOC signal when scanning the delay between the two inputs. A linear fit around the zero-crossing region gives a slope about 10 mV/fs.

2. Additional simulation results

2.1 Linear enhancement of soliton diffusion from increasing noise force. Since the soliton motion under quantum noise is small, we included a factor of 100 in the simulation to enhance the motion and avoid numerical artifacts (see main text and ref. [S1]). This section validates that this simulation method does not change the properties of quantum diffusion of solitons. It is verified that the CP soliton interaction dynamics remain the same and the diffusion coefficient (D) over the short time scale increases linearly when enhancing the noise force. To do this, we changed the noise enhancement factor in the simulation from 100 to $100\alpha_N$ while still normalizing the simulated relative soliton motion by 100 in the subsequent analysis.

Figure S2a shows the simulated Allan deviation ($\sigma_{\delta t}(\tau)$) of relative CP soliton motion for α_N=1, 4, and 16 (enhancing the noise force for both CP solitons). The analytical model giving the relative motion of two independent solitons is also plotted along with versions scaled by 2× and 4×. All the simulated $\sigma^2_{\delta t}(\tau)$ scale as Dτ over short times and roll-over at longer times due to the interaction between the solitons, as discussed in the main text. Moreover, at short times the Allan deviation of the α_N=4 and 16 cases are 2× and 4× (i.e., $\sqrt{\alpha_N}$ times) relative to the α_N=1 case. This shows the relative CP soliton motion is enhanced linearly with increasing noise force.

2.2 Noise in time domain and frequency domain. Figure S2b validates the simulation method of adding quantum noise in the time domain in the main text is equivalent to adding the quantum noise in the frequency domain. We add each frequency mode random photon fluctuation with a photon number variance of $\langle n(\mu,T)n(\mu',T')\rangle = \frac{\kappa T_R}{2}\delta(\mu-\mu',T-T')$ per round trip in the coupled LLEs, where n is the photon number and μ is the mode number with respect to the pumped mode. The simulated Allan deviation of the relative CP soliton motion forced by the

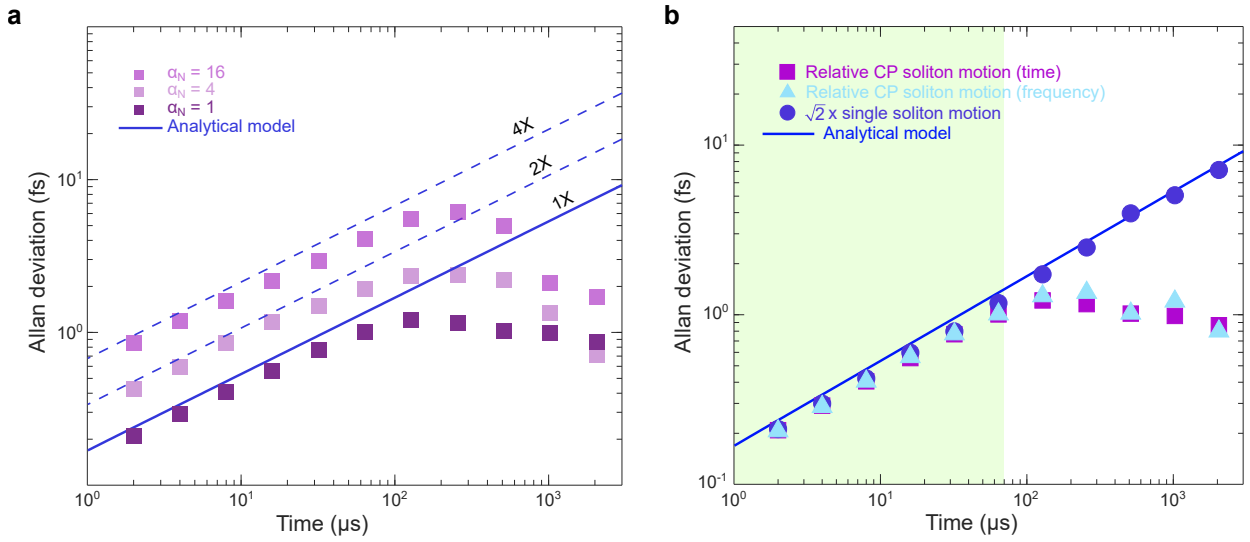

FIG. S2: **Enhancement of the diffusion coefficient and further validation of the simulation methods. a** Allan deviation versus time determined from the simulation with increasing amounts of added noise as determined by the parameter α_N (see text). The analytical model is also plotted (solid line) and with scaling factors corresponding to the noise added in the simulation (dashed lines). **b** The solid line gives the analytical prediction for the Allan deviation of two independent solitons, and the circles are the simulated Allan deviation of a single soliton (multiplied by $\sqrt{2}$ for comparison). The squares are the simulated relative CP soliton motion as in Fig. 1e of the main text where the noise is added in the time domain. For comparison, the triangles are the Allan deviation of the CP soliton motion when adding the quantum noise in the frequency domain.

noise added in the frequency domain is depicted by the triangles in Fig. S2b and matches the noise added in the time domain as in the main text (squares in Fig. S2b).

2.3 Relative CP soliton motion and single soliton motion. To further verify that the relative CP soliton motion simulated by the coupled LLEs represents the single soliton motion over short times, we compared it to the single soliton motion simulated using a single LLE with appropriate quantum noise terms. The single LLE without CP soliton interaction is written as

$$\frac{\partial A_1}{\partial T} = -\left(\frac{\kappa}{2} + i\delta\omega\right) A_1 - i\frac{\beta_2 L}{2T_R}\frac{\partial^2 A_1}{\partial t^2} + \frac{i\gamma A_1 L}{T_R}\int_{-\infty}^{+\infty} R(t')\,|A_1(T, t-t')|^2\,dt' + \sqrt{\frac{\kappa_e P_{\text{in}}}{T_R}} + F_1(t,T), \tag{S1}$$

which is the same as one of the coupled LLEs (eqns. 5, 6 in the main text) but without the coupling term (κ_b term). The simulated Allan deviation of single soliton motion (multipled by $\sqrt{2}$) is plotted as the circles in Fig. S2b, while the squares give the Allan deviation for the simulated relative CP soliton motion (Fig. 1e of the main text) using the coupled LLEs. The solid line is the analytical prediction for two non-interacting solitons. In the shaded region $\sigma_{\delta t}^2(\tau)$ scales as Dτ. Here, the CP solitons feature independent diffusive transport and their Allan deviation matches that of the single soliton motion (subject to the $\sqrt{2}$ scaling). For longer times, the interaction between the CP solitons causes their relative motion to deviate from the diffusive motion. A similar feature is also experimentally observed in Figs. 1e, f of the main text.

3. Simplification of the theoretical model

Comparing the first term $S_t^{(1)}$ and second term $S_t^{(2)}$ in Eqn. 1 at low offset frequencies $\omega \ll \kappa$ shows that,

$$\frac{S_t^{(1)}}{S_t^{(2)}} = \left(\frac{\pi\tau^2\kappa}{2\,|\beta_2|\,v_g}\right)^2 = \left(\frac{\pi\kappa}{4\delta\omega}\right)^2 \ll 1, \tag{S2}$$

where $\delta\omega$ is the detuning of the cavity resonant frequency relative to the pump frequency and is typically much larger than κ for stable soliton mode locking. In deriving this result the relationship $\gamma P = |\beta_2|/\tau^2 = 2\delta\omega/v_g$ [S2, S3] has been used where P is the peak soliton power in the cavity and $\gamma = n_2\omega_0/(cA_{\text{eff}})$ is the nonlinear coefficient (c is the light velocity in the vacuum, n_2 is the nonlinear index, and A_{eff} is the effective mode area).

A comparison of the second term $S_t^{(2)}$ and the third term $S_t^{(3)}$ in Eqn. 1 at low offset frequencies shows that,

$$\frac{S_t^{(2)}}{S_t^{(3)}} = \frac{|\beta_2|\, v_g}{3\omega\tau^2} = \frac{2\delta\omega}{3\omega} \gg 1 \tag{S3}$$

Therefore, the theoretical model can be simplified into Eqn. 2 of the main text.

[S1] R. Paschotta, Appl. Phys. B **79**, 153 (2004).
[S2] S. Wabnitz, Opt. Lett. **18**, 601 (1993).
[S3] T. Herr, V. Brasch, J. D. Jost, C. Y. Wang, N. M. Kondratiev, M. L. Gorodetsky, and T. J. Kippenberg, Nature Photonics **8**, 145 (2014).